Rare Metal Materials and Engineering
Volume 50, Issue 2, February 2021
Available online at www.rmme.ac.cn

Science Press

Cite this article as: Rare Metal Materials and Engineering, 2021, 50(2): 0511-0518.

ARTICLE

Electromechanical Properties of Lapped Joints of $Y_{0.5}Gd_{0.5}Ba_2Cu_3O_{7-z}$ Coated Conductors Joined with Lead-free Solders

Yang Gansong[1,2], Wang Wentao[2,3], Liu Lian[2,3], Wang Mingjiang[2,3], Tian Zhengjian[1,2], Zheng Qiutong[1,2], Zhao Yong[2,4]

[1] Key Laboratory of Advanced Technologies of Materials (Ministry of Education of China), School of Materials Science and Engineering, Southwest Jiaotong University, Chengdu 610031, China; [2] Superconductivity and New Energy R & D Center, Southwest Jiaotong University, Chengdu 610031, China; [3] Key Laboratory of Magnetic Suspension and Maglev Vehicle, Ministry of Education, School of Electrical Engineering, Southwest Jiaotong University, Chengdu 610031, China; [4] College of Physics and Energy, Fujian Normal University, Fuzhou 350117, China

Abstract: Due to the limited available piece length of $Y_{0.5}Gd_{0.5}Ba_2Cu_3O_{7-z}$ (YGdBCO) coated conductors (CCs), joints are inevitable for manufacturing high temperature superconducting (HTS) devices. The stable operation of HTS devices is largely determined by the quality of joints, because the electromechanical performance of joints is usually lower than that of original tapes. In this work, lead-free Sn42Bi58 solder was applied to make the lap joints for YGdBCO CCs. Compared with conventional Sn60Pb40 solder, lead-free Sn42Bi58 solder is environmentally friendly and soldering operation can be carried out at lower temperatures below 150 °C because the melting point is about 40 °C lower, thereby further reducing the CCs deterioration of property in joining process. The influence of loading pressure, pressurization speed and lapped length on the critical current, resistance and *n* values of the YGdBCO joints were investigated by measurement of voltage-current curve under self-field at liquid nitrogen temperature. Results show that by optimizing soldering technique, a 25 cm-long joint with quite low resistance of 4.35~5.58 nΩ and comparable critical current to virgin CCs can be repeatedly achieved under a pressure of 12.5 MPa and a pressurization speed of 50 N/s. The mechanical behavior of the joints under axial tension was studied and the critical axial tension force of single CCs and joint portion is 213 and 212 N, respectively. The above results show that compared with traditional soldering techniques, the robustness and reproducibility of the soldering joints with low resistance and high tension performance can be significantly improved by the joining technique based on this lead-free Sn42Bi58 solder, which offers another promising choice for joints manufacturing in the large-scale applications of YGdBCO CCs.

Key words: YGdBCO coated conductors; low-resistance joint; critical current; critical axial tension

$REBa_2Cu_3O_{7-z}$ (REBCO) high temperature superconducting (HTS) coated conductors (CCs) with high critical current densities and good mechanical properties are potentially applied in fault current limiter, magnetic energy storage and insert coil of nuclear magnetic resonance[1-3], which requires several or even more kilometers of REBCO CCs in a typical unit. Now the maximum length of 1 km can be achieved by currently advanced technologies, whereas it is still difficult to fabricate longer CCs with high and uniform critical current. Therefore, a large number of joints are required and the high quality joining of REBCO CCs, including low resistance, high mechanical properties and small AC loss, is essentially

Received date: February 09, 2020
Foundation item: National Natural Science Foundation of China (51271155, 51377138); Field Foundation of Pre-Research on Equipment (61409230502); Fundamental Research Funds for the Central Universities (2019XJ03, 2682015ZT11); Science and Technology Project in Sichuan Province (2017JY0057)
Corresponding author: Wang Wentao, Ph. D., Associate Professor, Superconductivity and New Energy R & D Center, Southwest Jiaotong University, Chengdu 610031, P. R. China, Tel: 0086-28-87600787, E-mail: wtwang@swjtu.edu.cn

important for manufacturing superconducting devices. In general, there are two types of joining techniques. One is non-superconducting joint, including soldering joint using low melting point solder materials[4-7] and diffusion joint by Ag diffusion at 400~500 °C in O_2 atmosphere[8-10] as well as newly developed joint by ultrasonic weld-solder hybrid method [11]. The other is superconducting joint by connecting REBCO superconducting layers directly in joint area[12,13]. Among these joints, soldering joint can be easily fabricated with simple device at temperatures below 250 °C in air. Compared with soldering joint, superconducting joint and Ag diffusion joint need to be heat treated at higher temperatures above 400 °C in O_2 or N_2 gas with more complicated equipment, although lower joint resistance can be obtained by these two techniques. Also, copper stabilizers need to be removed for these two joints, which reduces the mechanical properties of the superconducting CCs. Thus, soldering joint is still an alternative to large scale industrial manufacturing due to limited number of involved procedures and moderate temperature range.

In recent years, lead-free solders have attracted more attention in REBCO CCs joining by soldering method, because they are environmentally friendly and thus more suitable for large scale applications of HTS CCs. Michalcová et al[14,15] reported that the joint resistivity of 47.4~164 nΩ·cm^2 are achieved by traditional slow heating via hot plate and fast heating by high frequency inductor. They believed that this rapid heating method can prevent or minimize the growth of coarse Cu_6Sn_5 particles in Sn96.5Ag3.0Cu0.5 solders, which may be responsible for the reduced voids in cross section and lower joint resistance. Zhang et al[16] produced YBCO joint with resistance of 26.7 nΩ·cm^2 by Sn96.5Ag3.0Cu0.5 solder, and the axial tension behavior of the joint is comparable with that of virgin CCs. It is reported that soldering temperature should be kept below ~250 °C, especially for elongated processing time, to avoid possible degradation in superconductivity. The melting point of Sn96.5Ag3.0Cu0.5 is 217 °C, close to the tolerance temperature of REBCO CCs, which may deteriorate the properties of CCs during soldering process. Huang et al[17] reported that Bi introduction into Sn-based alloy can decrease the melting point of alloy and thus reduce the influence of high soldering temperature on the properties of CCs. However, the resistance obtained at liquid nitrogen temperature and self-field is usually variable between 25 and 1300 nΩ·cm^2 [18-25] by lead-free or lead-containing solders, because of different joining process and CCs. The robustness and reproducibility both need to be significantly improved to insure the stable operation of HTS devices. Compared with Sn96.5Ag3.0Cu0.5 and Pb-containing solder, lead-free Sn42Bi58 solder has much lower melting point of 138 °C, which can make the joining stage operate at lower temperatures, thus reducing the CCs deterioration during soldering process. But the joint soldering with Sn42Bi58 has seldom been thoroughly investigated, especially the soldering techniques or electromechanical behavior.

In this work, lead-free and low melting point Sn42Bi58 solder was used to join YGdBCO CCs by self-designed soldering device. For improving the robustness and reproducibility of joint, the influence of several crucial processing parameters including loading pressure, pressurization speed and joint length on the microstructure, resistance and critical current of joints was investigated by accurate control of pressure using universal testing machine. The pressure mainly affects the thickness of solder layer and the connectivity between solder and CCs. The various pressurization speeds correspond to different retention time at the melted state of solder, which has a distinct influence on the spreadability and micro-defects of solder. And the lapped length can easily adjust the joint area, thus changing the joint resistance. Therefore, these three parameters have a direct effect on the joint resistance and it is important to investigate them systematically. The behavior under different axial tension forces was also studied for the part of single tape and the joint portion of the same test piece by self-assembled tension device.

1 Experiment

1.1 YGdBCO coated conductors

4 mm-wide YGdBCO coated conductors (CCs) for joints were ST-4-E/100 version from Shanghai Superconductor and SCS4050 version from Superpower. These tapes have a laminated structure, mainly including a Hastelloy substrate, buffer stack, a superconducting layer and Ag/Cu stabilizers, as given in Fig.1a. Table 1 shows the specifications of the YGdBCO CCs used in this work.

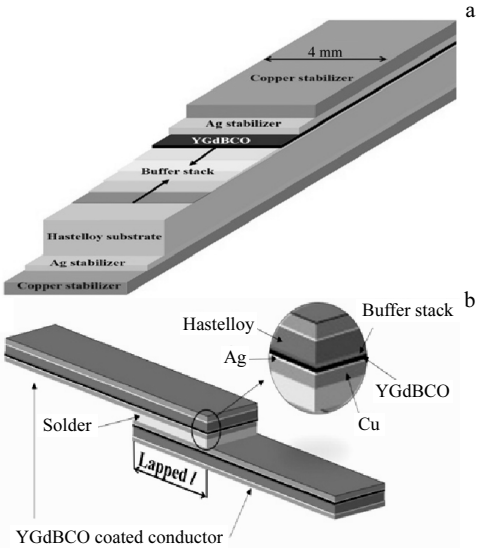

Fig.1 Schematic architecture of YGdBCO coated conductor (a) and lap joint (b)

Table 1 Specifications of YGdBCO tapes produced by superpower and SHSC

	IBAD/PLD YGdBCO CC	IBAD/MOCVD YGdBCO CC
Manufacturer	SHSC	Superpower
Type	ST-4-E/100	SCS4050
Structure	Ag/YBCO/LaMnO/ CeO_2/MgO/ Y_2O_3/Al_2O_3/Hasetlloy	Ag/YBCO/LaMnO/ Homo-epi MgO/IBAD MgO/Hastelloy
YBCO film, T/μm	~1	~1
I_c/A	165	100
Dimension, $T\times W$/mm	0.110×4.00	0.098×4.00
Substrate	Hastelloy	Hastelloy
Substrate, T/μm	50	50
Stabilizer, T/μm	Silver/1.5	Silver/2
Stabilizer, T/μm	Copper /30	Copper/20

T: thickness

1.2 Preparation of lapped joint

Compared with bridge and butt joints, lapped joints transmitting superconducting current with shorter path possess lower joint resistance and are easier to wind magnet. In this work, conductor pieces were joined with YGdBCO sides face-to-face, forming a lapped joint, as shown in Fig.1b. The samples were classified into ST-4-E/100-joints and SCS4050-joints. A self-designed welding device in Fig.2, consisting of temperature controller, thermocouple, hot plate, two stainless steel pressure plates and universal testing machine, was used to connect the YGdBCO CCs. The upper and the lower pressure plates with length of 32 and 40 cm, respectively, both have high smoothness and roughness less than 5 μm/100 mm and 0.8 μm, respectively. This welding device can make long joint up to 32 cm and accurately control the pressure and the pressurization speed applied on samples, ensuring stable mechanical pressure subjected on the joints before the solidification of solders.

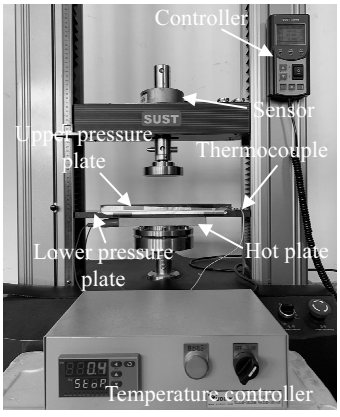

Fig.2 Self-designed soldering device for YGdBCO lap joint

The fabrication procedure of the samples mainly has five steps, including tape cleaning, pressure plate preheating, solder coating, pressurization and pressure plate cooling. First, the tapes were cleaned with ethanol to eliminate organics and other impurities. Then the two pressure plates wrapped with tin foil were placed on a hot plate and heated to ~145 °C. This soldering temperature is few higher than the melting point of Sn42Bi58 solder. When the temperature was stable, flux and the solder were successively coated on the lapped area. The major role of the flux is to promote wetting by cleaning the metal oxides and other contaminants from the surface to be soldered. The joint was prepared by placing another conductor piece face-to-face on the heated piece and subjected to an appropriate pressure applied by a universal testing machine. The lapped length was 5~30 cm; thus, the total length of the sample with joint was 15~40 cm. The pressure was 2.5~15 MPa, and the pressurization speed was 5~70 N/s, which was preset before putting pressure on joint and controlled by the servo motor of the universal testing machine. Finally, the joint was obtained after the pressure plate was cooled down to room temperature. All samples, varying in pressure, pressurization speed and lapped length, were subjected to the same heat treatment during the joining process.

1.3 Measurement and analysis

In order to investigate the electromechanical performance of the samples, *V-I* characteristic curves of the samples were measured by four-probe transport method at liquid nitrogen temperature (77 K) and self-field. The Sorensen SFA series of high-power DC current source was used to generate 3 A/s current, and the Keithley 2182A digital nanovoltmeter was used to measure voltage. The joint resistance, critical current and n value were obtained from the *V-I* characteristic curves. The joint resistance is equivalent to the slope of the *V-I* curve and calculated by the governing equation of the *V-I* curve:

$$V=R_cI+V_c(I/I_c)^n \quad (1)$$

where V is the voltage, I is the current, R_c is the joint resistance, V_c is the criterion voltage of 1 μV/cm to determine the transition of the samples, I_c is the critical current, n indicates the rate at which the superconducting materials transform from a superconducting state to a normal state, which is related to the uniformity of the material.

The microstructures of the joints were observed by optical microscope (OM) and scanning electron microscope (SEM). The cross section of the joint fixed by acrylic was sanded by the abrasive paper with different mesh of 600~10000, and was polished with diamond grinding paste. The axial tensile force of the samples was tested by a self-assembled tensile test system based on a universal testing machine.

2 Results and Discussion

2.1 Joint resistance as a function of loading pressure

The pressure applied during soldering stage, directly determining the microstructure and connectivity of joint, is one of

the crucial processing parameters. The influence of pressure on the resistance of SCS4050-joints was investigated at the same lapped length and pressurization speed. As can be seen in Fig.3a, the lowest resistance of 31.25 nΩ was obtained for 5 cm-long joint at the pressure of 12.5 MPa. When the pressure is below 12.5 MPa, the resistance decreases with increasing the pressure. But the resistance slightly increases when the pressure is above 12.5 MPa. As we know, resistance is defined as follows:

$$R = \rho \frac{L}{S} \quad (2)$$

where R is the joint resistance, ρ is the total specific resistance of the joint region including the contact resistances between different materials and the material resistivities, L is the distance between two superconducting layers, S is the lapped area. As shown in Fig.3a, the solder thickness reduces from 30 to 2 μm with increasing the loading pressure up to 12.5 MPa, resulting in a L decrease according to Eq.(2). So R reduces gradually with the increase of the pressure. The cross sections of the joints under various pressures are shown in Fig.4a~4f. The thickness changes of solder layers can be clearly observed by optical microscope images in this figure. However, when the solder is thin enough under the pressure above 12.5 MPa, the main factors that determine the joint resistance are the own

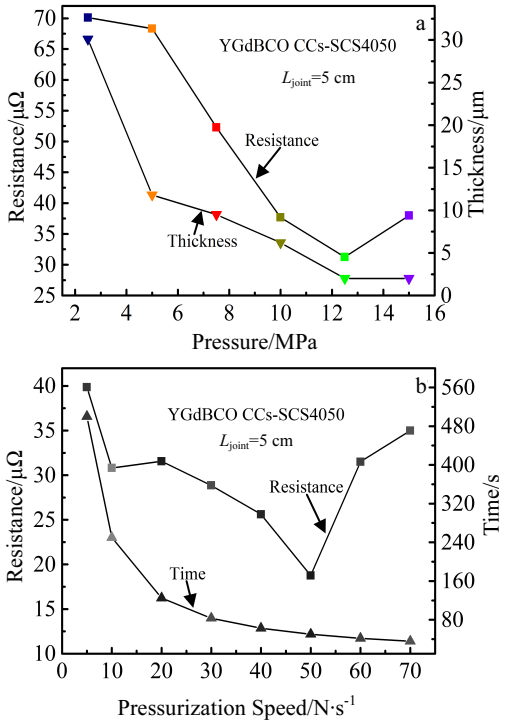

Fig.3 Influence of pressure on the resistance and the thickness of solder layer (a) and effect of pressurization speed on the resistance and pressurization time (b) of SCS4050-YGdBCO joints

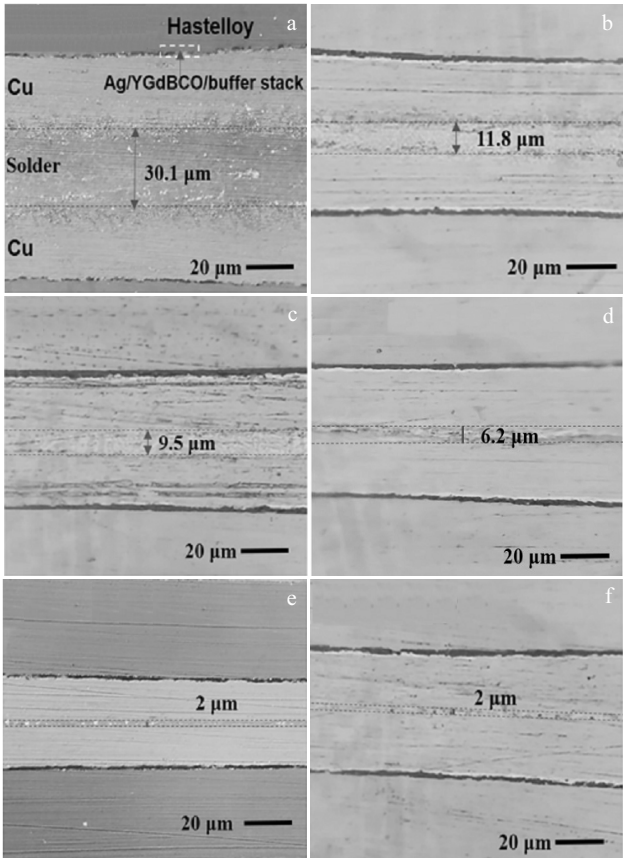

Fig.4 OM images of cross-section of SCS4050-YGdBCO joints under the pressure of 2.5 MPa (a), 5 MPa (b), 7.5 MPa (c), 10 MPa (d), 12.5 MPa (e) and 15 MPa (f)

resistance of metal stabilizers and solder as well as the contact resistance between different layers. This resistance is different for the coated conductors produced by different manufacturers or various conductor batches from the same manufacturer. Therefore, the results and discussion in this work are based on the same batch of conductors fabricated by the same manufacturer.

2.2 Joint resistance as a function of pressurization speed

The pressurization speed in soldering process has also a big influence on the joint resistance apart from the loading pressure, because it affects the distribution and purity of solder in the lapped region. In this work, the SCS4050-joint resistance as a function of the pressurization speed was firstly investigated with a constant set of lapped length (5 cm) and pressure (12.5 MPa). As shown in Fig.3b, the lowest resistance of 18.76 nΩ is achieved at the pressurization speed of 50 N/s. When the pressurization speed is below 50 N/s, the resistance decreases with increasing the pressurization speed. While the resistance distinctly increases with further rising the pressurization speed above 50 N/s. Zhang et al[26] reported that melted Sn-Bi alloy can react with copper at interface, generating intermetallic compounds Cu_3Sn and

Cu_6Sn_5. These two impurities may contribute to the joint resistance. With a pressurization speed lower than 50 N/s, it takes 50~500 s to reach the set pressure (12.5 MPa), as shown in Fig.3b, so there is enough time for this reaction to form more Cu_3Sn and Cu_6Sn_5 in the joint region. However, the solder may not be squeezed out evenly and cannot spread uniformly on the conductor piece within a short time of 41.7 s (60 N/s) and 35.7 s (70 N/s) in Fig.3b, thus generating more microdefects and increasing interface resistance between solder and copper layers, although this short-time retention can reduce the amount of intermetallic compounds. Accordingly, the low-resistance joint can be achieved by improving the spreadability of solder and suppressing the generation of impurities through tuning the pressurization speed.

2.3 Electrical properties for joints with different lapped lengths

According to Eq.(2), joint resistance can further decrease by increasing the lapped area of joint. In this work, the lapped area was enlarged by prolonging the joint length, since the width of the conductors (4 mm) is constant. The electrical properties were studied for the ST-4-E/100- and SCS4050-joints with 5~30 cm lapped length, based on the same pressure (12.5 MPa) and pressurization speed (50 N/s). Fig.5 shows the *V-I* curves of these joints. As can be clearly seen from the insets, the critical currents I_c are quite close for the virgin CCs and the joints, but *n* values reduce after the soldering process. It means that the current-carrying capability of the joints is comparable to that of the virgin one. The reduced *n* values are due to the insertion of a non-superconducting solder layer. In addition, it can be known from the slope of *V-I* curves that the resistance of two types of joints changes with lapped lengths.

The relationship between the lapped length and the resistance was systematically studied through repeatedly making a series of ST-4-E/100- and SCS4050-joints. Fig.6 plots the joint resistance as a function of the joint lapped length. It is shown that the resistance reduces with increasing the joint lapped length, and the resistance changes slightly with further increasing the joint lapped length from 25 cm to 30 cm. Also, the SCS4050-joints have lower average resistance compared with the ST-4-E/100-joints. The lowest resistance is 4.35 and 6.88 nΩ for the 25 cm-long SCS4050-joint and 30 cm-long ST-4-E/100-joint, respectively,. The corresponding joint resistivity is 43.5 nΩ·cm^2 for the SCS4050-joint, which is lower than the best value of 67 nΩ·cm^2 reported by Michalcová[14]. They thought that the differences may be caused by the much thicker soldering layer in their samples which was in range of 85~100 μm. Since the resistance for 25 cm- and 30 cm-joint is already extremely low, it is difficult to distinctly reduce the resistance by further increasing the lapped length. It may be necessary to further optimize soldering parameters to reduce the microdefects in solder layers or further decrease the contact resistance

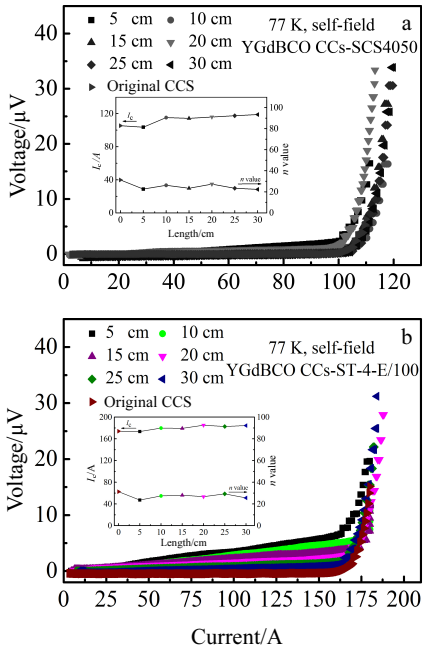

Fig.5 *V-I* performance of SCS4050- (a) and ST-4-E/100- (b) YGdBCO original tapes and joints with different lapped lengths (insets are I_c and *n* values corresponding to different lapped lengths)

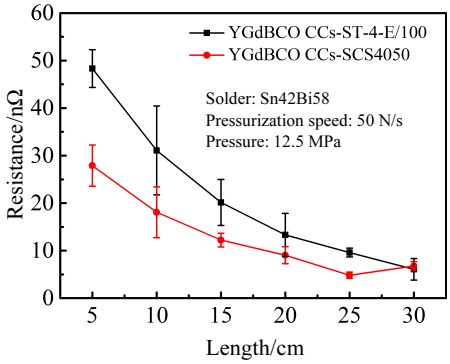

Fig.6 Lapped length dependence of joint resistance for SCS4050- and ST-4-E/100-YGdBCO joints

between Cu and solder layers. As we know, the joint resistance is mainly originated from the own resistance of Cu, Ag and solder layer, and the contact resistance between different materials. The calculation formula is:

$$R_j=2R_{YGdBCO\text{-}Ag}+2R_{Ag\text{-}Cu}+2R_{Cu\text{-}Solder}+2R_{Ag}+2R_{Cu}+R_{Solder} \quad (3)$$

where R_j is the joint resistance; $R_{YGdBCO\text{-}Ag}$ is the contact resistance between YGdBCO superconducting layer and Ag layer; $R_{Ag\text{-}Cu}$ is the contact resistance between Ag and Cu layers, $R_{Cu\text{-}Solder}$ is the contact resistance between Cu and solder layers; R_{Ag}, R_{Cu} and R_{Solder} are the own resistance of Ag, Cu and solder, respectively. Therefore, the resistance differences for two types joints may be due to different contact resistance

($R_{YGdBCO-Ag}$, R_{Ag-Cu}, $R_{Cu-Solder}$) caused by various materials structures and preparation methods of the coated conductors. And different roughness of Cu layers for two types conductors results in different spreadability of solder on the Cu layers, which may be another reason for the resistance differences.

A series of SCS4050-joints with comparable properties were obtained by the optimized soldering technology and the resistance of six joints is shown in Table 2. All the joints soldered with the same batch of CCs display low resistance in the range of 4.35~5.58 nΩ on the basis of the same joint width (4 mm) and length (25 cm). The corresponding resistivity is 43.5~55.8 nΩ·cm^2 for these joints, which is very different from the big resistance difference for the SCS4050-joints with the same batch reported by Lu[24]. Also, dense and uniformly distributed solder layer was observed by scanning electron microscope (SEM), as shown in Fig.7. The above results indicate that robustness and reproducibility of the joints joined with lead-free Sn42Bi58 are improved by optimizing the pressure, the pressurization speed and the lapped length based on the pressure plates with high smoothness and low roughness, which is of great importance for the industrial production of soldering joints and large-scale HTS applications.

2.4 Axial tension behavior of virgin tape and joints

The mechanical property is another important issue for the practical HTS applications apart from the low joint resistance and high critical current. In this part, the *V-I* behavior of SCS-4050 joints under different axial tension was investigated for the part of single CCs and the joint portion of the same test piece with lapped length of 5 cm because of their lower resistances under the same soldering process compared with ST-4-E/100 joints. As can be seen in Fig.8, I_c values for the unjoined and joined parts are similar to those of single CCs when the axial tension is below 210 N. The I_c value decreases distinctly with increasing the axial tension to 220 N and about 45% I_c deterioration is found in both parts of this sample when the axial tension further rises to 230 N. It is worthy to point out that the joint resistance does not change under the axial tension even when I_c distinctly reduces to about 60 A, according to the unchanged initial slopes of the *V-I* curves in Fig.8b. This means that the joining layers are still undamaged when the YGdBCO superconducting layer is partially damaged under the axial tension, showing the reliability and robustness of the soldering joint with this lead-free Sn42Bi58 solder.

The part of single CCs and the joint portion were subjected to loading and unloading procedure in order to check the reversibility of I_c. 99% recovery is used as the reversibility criterion when the load is released. As can be seen in Fig.9, the load corresponding to the 99% recovery in the unjoined part is 190 N, larger than 180 N in the joined area. The critical axial tension force defined by the 95% retention of I_c is 213 and 212 N for the unjoined and joined area, respectively. It shows that the critical axial tension for 95% retention in the joint is comparable to that in the single CCs, indicating the good axial tension properties of the joint. Although the joints with low resistance and good axial tension behavior have been repeatedly achieved using lead-free Sn42Bi58 solder in this

Table 2 Resistance of jointed samples at 77 K

Manufacturer & type	Sample	Width/ cm	Overlap length/cm	I_c/ A	R_j/ nΩ	R_j·S_j/ nΩ·cm^2
Superpower SCS4050	1	0.4	25	117.8	4.5	45
	2	0.4	25	115.7	4.35	43.5
	3	0.4	25	114.9	4.81	48.1
	4	0.4	25	114.6	5.58	55.8
	5	0.4	25	116.3	4.62	46.2
	6	0.4	25	114.1	5.14	51.4

R_j: joint resistance; S_j: lapped area

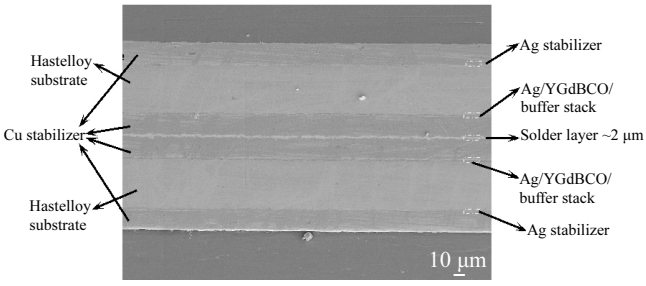

Fig.7 SEM image of the cross-section of SCS4050-YGdBCO joints fabricated under optimal parameters

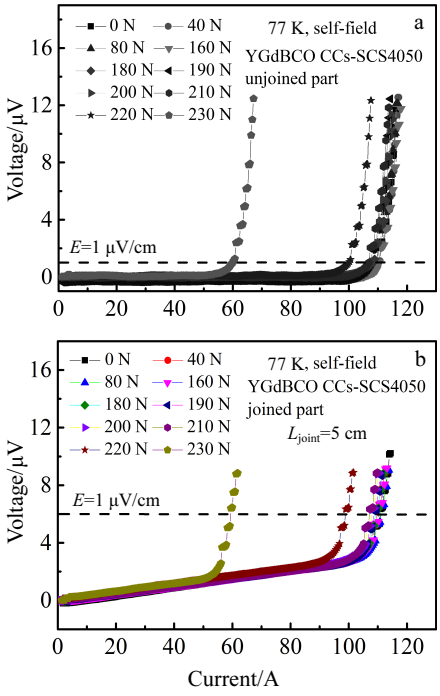

Fig.8 *V-I* characteristics of unjoined (a) and joined (b) parts for the same test piece (SCS4050-YGdBCO) under axial tension

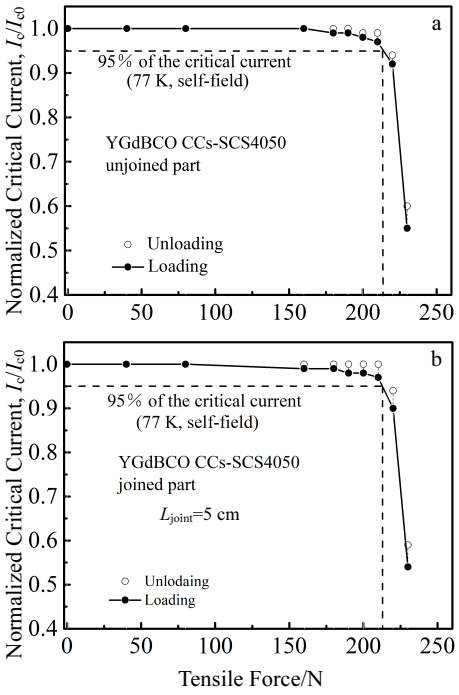

Fig.9 Dependence of normalized I_c of the unjoined (a) and joined (b) part for the same test piece (SCS4050-YGdBCO) on axial tension

work, the delamination strength and bending performance of the joints are necessary to be studied in future for the further promotion of practical applications of REBCO high temperature superconducting coated conductors.

3 Conclusions

1) SCS4050- and ST-4-E/100-joints for YGdBCO coated conductors can be fabricated using lead-free and low melting point Sn42Bi58 solders by self-designed welding device.

2) The joint resistance can be reduced by thinning solder layer, suppressing impure Cu_3Sn and Cu_6Sn_5 formation in joint portion, improving the spreadability of solder and enlarging lapped area.

3) The low resistance of 4.35~5.58 nΩ for 25 cm-long joints is repeatedly achieved with the optimal soldering technique at pressure of 12.5 MPa and pressurization speed of 50 N/s.

4) The joined parts display comparable critical axial tension force of 212 N to the single CCs, showing good behavior under axial tension load.

5) A practical soldering approach using lead-free Sn42Bi58 solders is developed for low-resistance joints of YGdBCO coated conductors, and it can be potentially applied in the manufacturing of high temperature superconducting magnets.

References

1 Yang Q, Le Blond S, Liang F *et al*. *IEEE Transactions on Applied Superconductivity*[J], 2017, 27(4): 3 800 805

2 Yao W, Jiang L, Fang J *et al*. *International Journal of Electrical Power & Energy Systems*[J], 2016, 78(1): 555

3 Yokoyama S, Lee J, Imura T *et al*. *IEEE Transactions on Applied Superconductivity*[J], 2017, 27(4): 4 400 604

4 Zhang S, Li F, Yang G *et al*. *IEEE Transactions on Applied Superconductivity*[J], 2019, 29(5): 8 800 807

5 Martino E, Bocchi M, Angeli G *et al*. *IEEE Transactions on Applied Superconductivity*[J], 2018, 28(1): 5 600 204

6 Xie Y, Ouyang Z, Shi L *et al*. *IOP Conference Series: Materials Science and Engineering*[J], 2017, 171: 12 155

7 Sohn M H, Kim S W, Baik S K *et al*. *IEEE Transactions on Applied Superconductivity*[J], 2003, 13(2): 1764

8 Mori N, Yoshida J, Maebatake T *et al*. *Journal of Physics: Conference Series*[J], 2010, 234(2): 22 023

9 Maebatake T, Ichinose Y, Yamada K *et al*. *Physica C: Superconductivity and Its Applications*[J], 2011, 471(21): 987

10 Pan Y, Sheng J, Wu W *et al*. *IEEE Transactions on Applied Superconductivity*[J], 2017, 27(4): 6 601 905

11 Shin H S, Jung C H. *IEEE Transactions on Applied Superconductivity*[J], 2017, 27(4): 6 602 105

12 Park Y J, Lee M W, Oh Y K *et al*. *Superconductor Science and Technology*[J], 2014, 27: 85 008

13 Park Y J, Lee M W, Ann H *et al*. *NPG Asia Materials*[J], 2014, 6: 98

14 Michalcová E, Gömöry F, Frolek L *et al*. *IEEE Transactions on Applied Superconductivity*[J], 2016, 26(3): 8 801 104

15 Drienovsky M, Michalcová E, Pekarčíková M *et al*. *IEEE Transactions on Applied Superconductivity*[J], 2018, 28(4): 6 601 305

16 Liu W, Zhang X, Liu Y *et al*. *IEEE Transactions on Applied Superconductivity*[J], 2014, 24(6): 6 600 805

17 Huang M L, Zhou Q, Zhao N *et al*. *Journal of Materials Science: Materials in Electronics*[J], 2013, 24(7): 2624

18 Seino Y, Ito S, Hashizume H. *IEEE Transactions on Applied Superconductivity*[J], 2014, 24(3): 4 602 105

19 Shin H S, Dedicatoria M J. *IEEE Transactions on Applied Superconductivity*[J], 2010, 20(3): 1541

20 Chang K S, Jo H C, Kim Y J *et al*. *IEEE Transactions on Applied Superconductivity*[J], 2011, 21(3): 3005

21 Bagrets N, Weiss K P, Nast R *et al*. *IEEE Transactions on Applied Superconductivity*[J], 2018, 28(4): 6 600 204

22 Zheng J, Ma H, He R *et al*. *IEEE Transactions on Applied Superconductivity*[J], 2017, 27(5): 6 603 706

23 Preuss A, Fietz W H, Immel F *et al*. *IEEE Transactions on Applied Superconductivity*[J], 2018, 28(4): 6 601 105

24 Lu J, Han K, Sheppard W R *et al*. *IEEE Transactions on Applied Superconductivity*[J], 2011, 21(3): 3009

25 Bagrets N, Augieri A, Celentano G *et al*. *IEEE Transactions on Applied Superconductivity*[J], 2015, 25(3): 6 602 705

26 Zhang Q, Zou H, Zhang Z. *Scientia Sinica Technologica*[J], 2012, 42(1): 13 (in Chinese)

无铅焊料制备的 $Y_{0.5}Gd_{0.5}Ba_2Cu_3O_{7-z}$ 涂层超导带材搭接接头的机电性能研究

杨淦淞[1,2]，王文涛[2,3]，刘　连[2,3]，王明江[2,3]，田正健[1,2]，郑秋瞳[1,2]，赵　勇[2,4]

(1. 西南交通大学 材料科学与工程学院 材料先进技术教育部重点实验室，四川 成都 610031)

(2. 西南交通大学 超导与新能源研发中心，四川 成都 610031)

(3. 西南交通大学 电气工程学院 磁浮技术与磁浮列车教育部重点实验室，四川 成都 610031)

(4. 福建师范大学 物理与能源学院，福建 福州 350117)

摘　要：由于单根 $Y_{0.5}Gd_{0.5}Ba_2Cu_3O_{7-z}$ (YGdBCO)涂层超导带材的长度有限，因此在制造高温超导(HTS)器件时不可避免地需要接头。HTS设备的稳定运行在很大程度上取决于接头的品质，因为接头的机电性能通常低于母材。本研究应用 Sn42Bi58 焊料制作 YGdBCO 涂层超导带材搭接接头。与传统的 Sn60Pb40 焊料相比，无铅 Sn42Bi58 焊料对环境友好，且熔点降低了 40 ℃，因此可在低于 150 ℃的低温下进行焊接操作，有助于抑制超导带材在连接过程中的性能下降。通过测量自场和液氮温度下的电压-电流曲线，研究了加载压力，加压速度和搭接长度对 YGdBCO 接头临界电流，电阻和 *n* 值的影响。通过优化焊接技术，可在 12.5 MPa 的压强和 50 N/s 的加压速度下重复获得与母材临界电流相当的 25 cm 长的低阻接头，其电阻为 4.35~5.58 nΩ。还对轴向拉伸作用下接头的力学行为进行了研究，单根带材和接头部分的临界轴向拉伸力分别为 213 和 212 N。 上述结果表明，与传统焊接技术相比，采用优化的无铅 Sn42Bi58 焊料制备低电阻、高拉伸特性的焊接接头的稳定性和重复性明显提升，为 YGdBCO 超导带材大规模运用的接头连接提供了一种有前景的选择。

关键词：YGdBaCuO 涂层超导体；低电阻接头；临界电流；临界轴向拉伸

作者简介： 杨淦淞，男，1995 年生，硕士，西南交通大学超导与新能源研发中心，四川 成都 610031，电话：028-87600787，E-mail: 986531962@qq.com